Journal of Communications and Information Networks, Vol.2, No.4, Dec. 2017
DOI: 10.1007/s41650-017-0035-5

Research paper

Special Focus on Optical Wireless Communication

Enhanced asymmetrically clipped DC biased optical OFDM for intensity-modulated direct-detection systems

Ruowen Bai*, Jiaxuan Chen, Tianqi Mao, Zhaocheng Wang

Tsinghua National Laboratory for Information Science and Technology (TNList), Department of Electronic Engineering, Tsinghua University, Beijing 100084, China

* Corresponding author, Email: brw15@mails.tsinghua.edu.cn

Abstract: In this paper, we propose an EADO-OFDM (Enhanced Asymmetrically Clipped DC Biased Optical Orthogonal Frequency Division Multiplexing) method for IM/DD (Intensity-Modulated Direct-Detection) optical systems, in which the AV-DCO-OFDM (Absolute Valued DC Biased Optical OFDM) symbols on the even subcarriers and ACO-OFDM (Asymmetrically Clipped Optical OFDM) symbols on the odd subcarriers are combined for simultaneous transmission. Moreover, we discuss the PDF (Probability Density Function) and electrical SNR (Signal to Noise Ratio) of the symbols, which are utilized to estimate the BER (Bit Error Ratio) performance and overall performance of EADO-OFDM. The Monte Carlo simulation results have validated the theoretical analysis and have also confirmed the EADO-OFDM is attractive considering the following benefits. Firstly, EADO-OFDM is more energy efficient compared to the power-efficient DCO-OFDM (DC Biased Optical OFDM), since the required DC bias is smaller when appropriate constellation size combinations are chosen. In addition, EADO-OFDM performs better than the conventional ADO-OFDM (Asymmetrically Clipped DC Biased Optical OFDM), because the absolute value operation causes no clipping distortion.

Keywords: orthogonal frequency division multiplexing, intensity modulation with direct detection, optical wireless communications, visible light communications, absolute value operation

Citation: R. W. Bai, J. X. Chen, T. Q. Mao, et al. Enhanced asymmetrically clipped DC biased optical OFDM for intensity-modulated direct-detection systems [J]. Journal of communications and information networks, 2017, 2(4): 36-46.

1 Introduction

IM/DD systems are utilized widely in OWC (Optical Wireless Communication)[1,2], fiber-optic communication[3], amplitude modulated RF (Radio Frequency) wireless communication[4], and broadband wireline transmission[5]. In IM/DD OWC systems, the transmitted electrical signal is modulated onto the instantaneous power of an optical emitter such as LED (Light-Emitting Diode) or LD (Laser Diode). Thus the time-domain signals should be real-valued and nonnegative[1,2,6].

Manuscript received Apr. 25, 2017; accepted Jul. 04, 2017
This work is supported in part by National Key Basic Research Program of China (No. 2013CB329200), in part by Shenzhen Subject Arrangements (No. JCYJ20160331184124954), in part by Shenzhen Peacock Plan (No. 1108170036003286), in part by Guangdong Science and Technology Planning Project (No. 2014B010120001), in part by Shenzhen Fundamental Research Project (No. JCYJ20150401112337177), in part by Shenzhen Visible Light Communication System Key Laboratory (No. ZDSYS20140512114229398), and in part by EPSRC Funded Projects (EP/N004558/1, EP/N023862/1).

OFDM (Orthogonal Frequency Division Multiplexing) is not only a popular physical layer scheme in RF communication systems, but also a promising candidate for IM/DD OWC systems due to its inherent benefits like high spectral efficiency and resistance to frequency-selective channels[7]. Unlike RF communication, the input OFDM symbols for OWC should meet the Hermitian symmetry constraint to make the time-domain signals real-valued[8]. Meanwhile, to make the signals nonnegative, many optical OFDM schemes have been developed, including DCO-OFDM and ACO-OFDM. In DCO-OFDM, a DC bias is added to the bipolar time-domain signals, and all the remaining negative signals are clipped at zero. This is easy to implement but results in clipping distortion and performance degradation. In addition, the DC bias consumes much power, which reduces the energy efficiency. In ACO-OFDM, which is proposed for its high energy efficiency, only the odd subcarriers modulate the useful symbols, and the time-domain signals have antisymmetry property. Therefore, the negative parts can be clipped without losing any information[8,9]. However, ACO-OFDM is spectrally inefficient, since only half of the subcarriers are employed. ADO-OFDM has been proposed to overcome the drawbacks of DCO-OFDM and ACO-OFDM, in which DCO-OFDM symbols are modulated onto the even subcarriers while ACO-OFDM symbols are modulated onto the odd subcarriers[10,11]. ADO-OFDM possesses the advantages of both ACO-OFDM and DCO-OFDM; however, it is still degraded by the clipping distortion caused by the DCO-OFDM signal generating process.

In this paper, we propose an EADO-OFDM method, in which ACO-OFDM symbols are modulated onto the odd subcarriers and AV-DCO-OFDM symbols are modulated onto the even subcarriers. At the receiver, the ACO-OFDM symbols are first demodulated from the odd subcarriers. Then the ACO-OFDM time-domain signals are reconstructed and removed from the received signals. Similar to Ref. [12], ISEA (Iterative Signs Estimation Algorithm) is utilized to estimate the signs of the AV-DCO-OFDM time-domain signals. With the aid of the signs, we could detect the AV-DCO-OFDM symbols on the even subcarriers. Compared to the conventional ADO-OFDM, EADO-OFDM could achieve better BER performance for high SNR, because the absolute value operation causes no clipping distortion. Besides, compared to the power-efficient DCO-OFDM proposed in Ref. [12], EADO-OFDM is more energy efficient, since the DC bias required is smaller when appropriate constellation size combinations are chosen.

The remainder of this work is organized as follows. In section 2, the transceiver designs of the EADO-OFDM are proposed. In section 3, the PDF, electrical SNR, optical power allocation, and computational complexity analysis are discussed. In section 4, the Monte Carlo simulations are presented to validate the theoretical analysis and are compared to the conventional ADO-OFDM and the power-efficient DCO-OFDM. The conclusions are drawn in section 5.

2 Proposed EADO-OFDM

2.1 EADO-OFDM transmitter

The block diagram of the transmitter for an OWC system with N subcarriers is shown in Fig. 1. As depicted in the figure, Hermitian symmetry is imposed on the N subcarriers to generate real-valued time-domain signals, where we have $X_k = X^*_{N-k}$, and X_0 and $X_{N/2}$ are set to zero. Thus, the AV-DCO-OFDM frequency-domain symbol vector $\boldsymbol{X}$ on the even subcarriers is given by

$$\begin{aligned}\boldsymbol{X} = \big[&0, 0, X_2, 0, \cdots, X_{N/2-2},\\ &0, 0, 0, X^*_{N/2-2}, \cdots, X^*_2, 0\big],\end{aligned} \tag{1}$$

where X_k is the complex-valued symbol on the kth ($2 \leqslant k \leqslant N/2-2$) subcarrier, according to the chosen QAM (Quadrature Amplitude Modulation) constellation. The constellation size is assumed to be M_1.

The time-domain signals $\{x_n\}$, which are obtained after an IFFT (Inverse Fast Fourier Trans-

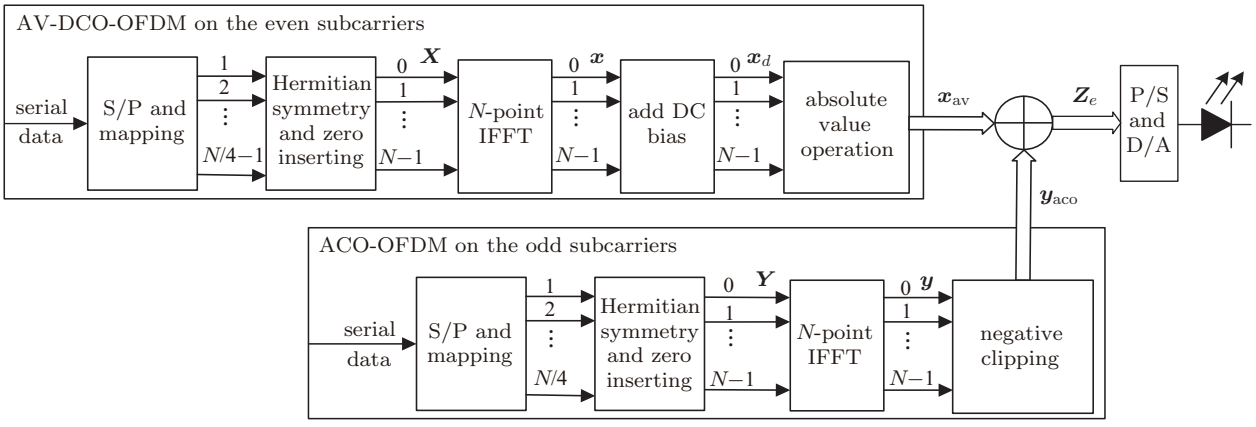

Figure 1 Block diagram of an EADO-OFDM transmitter

form) block, are given by

$$x_n = \frac{1}{\sqrt{N}} \sum_{k=0}^{N-1} X_k \exp\left(\mathrm{j}\frac{2\pi}{N} nk\right), \quad 0 \leqslant n \leqslant N-1. \tag{2}$$

According to Refs. [10,11], the signals $\{x_n\}$ have a symmetry property.

To ensure that the signals are nonnegative, a DC bias is added, and we have

$$x_{d,n} = x_n + B_{\mathrm{DC}}, \tag{3}$$

where the bias is given by $B_{\mathrm{DC}} = \mu\sigma_D$ and σ_D is the standard deviation, given by $\sigma_D = \sqrt{E\{x_n^2\}}$ with $E\{\cdot\}$ denoting expectation operation. μ is a proportionality constant. As in Ref. [12], the bias-index is often defined as $\beta = 10\lg(1+\mu^2)$ dB.

Usually, a DC bias cannot ensure that all the signals are nonnegative. Therefore, an absolute value operation is employed and the AV-DCO-OFDM time-domain signals $\{x_{\mathrm{av},n}\}$ are obtained. They are given by

$$x_{\mathrm{av},n} = |x_{d,n}| = x_n + B_{\mathrm{DC}} + w_a, \tag{4}$$

where $|\cdot|$ denotes an absolute value operator and w_a is the noise component caused by the absolute value operation, given by

$$w_{a,n} = \begin{cases} -2(x_n + B_{\mathrm{DC}}), & x_n < -B_{\mathrm{DC}}, \\ 0, & x_n \geqslant -B_{\mathrm{DC}}. \end{cases} \tag{5}$$

Due to the symmetry property of $\{x_n\}$, the signals $\{x_{\mathrm{av},n}\}$ are also symmetric, and are given by

$$x_{\mathrm{av},n} = x_{\mathrm{av},n+N/2}, \quad 0 \leqslant n \leqslant N/2-1. \tag{6}$$

Note that the signs of $x_{d,n}$ could be estimated successfully for high SNR using the ISEA algorithm proposed in Ref. [12]; therefore, compared to the conventional DCO-OFDM, no information is lost.

Besides, the ACO-OFDM symbol vector $\boldsymbol{Y}$ modulated on the odd subcarriers, is also constrained by Hermitian symmetry, which is given by

$$\boldsymbol{Y} = \left[0, Y_1, 0, Y_3, \cdots, Y_{N/2-1}, 0, Y_{N/2-1}^*, \cdots, Y_1^*\right], \tag{7}$$

where Y_k is a complex-valued symbol on the kth $(1 \leqslant k \leqslant N/2-1)$ subcarrier, according to the chosen QAM constellation with size M_2.

Similarly, $\boldsymbol{Y}$ is converted by an N-point IFFT to yield the time-domain signals $\{y_n\}$, which have an antisymmetry property as given by[9]

$$y_n = -y_{n+N/2}, \quad 0 \leqslant n \leqslant N/2-1. \tag{8}$$

Due to the antisymmetry property, the negative part of $\{y_n\}$ could be clipped without losing any information, and the time-domain signals $\{y_{\mathrm{aco},n}\}$ are obtained as[11]

$$y_{\mathrm{aco},n} = \frac{1}{2} y_n + c_{\mathrm{aco},n}, \quad 0 \leqslant n \leqslant N-1, \tag{9}$$

where $c_{\mathrm{aco},n}$ denotes the clipping distortion given by

$$c_{\mathrm{aco},n} = \frac{1}{2}|y_n|. \tag{10}$$

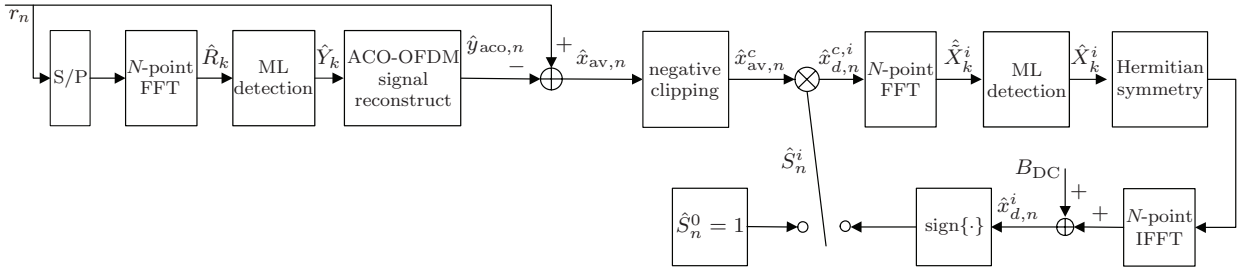

Figure 2 Block diagram of an EADO-OFDM receiver

Finally, the EADO-OFDM time-domain signals are obtained by adding $y_{\mathrm{aco},n}$ to $x_{\mathrm{av},n}$ as shown in Fig. 1, which are given by

$$z_{e,n} = x_{\mathrm{av},n} + y_{\mathrm{aco},n}, \quad 0 \leqslant n \leqslant N-1. \tag{11}$$

After the P/S (Parallel to Serial) and D/A (Digital to Analog) conversions, the continuous-time analog signal $z_e(t)$ is utilized to drive the optical emitter.

2.2 EADO-OFDM receiver

The block diagram of an EADO-OFDM receiver is shown in Fig. 2. At the receiver, a flat channel with perfect equalization is assumed, and the shot noise and thermal noise are commonly modeled as AWGN (Additive White Gaussian Noise)[10,11]. Thus, the received signals $\{r_n\}$ are given by

$$\begin{aligned} r_n &= z_{e,n} + w_{g,n} \\ &= x_{\mathrm{av},n} + \frac{1}{2}y_n + c_{\mathrm{aco},n} + w_{g,n},\ 0 \leqslant n \leqslant N-1, \end{aligned} \tag{12}$$

where $w_{g,n}$ denotes the sample of AWGN with zero mean and variance of σ_g^2.

After S/P (Serial to Parallel) conversion and N-point FFT (Fast Fourier Transform), the frequency-domain symbols are generated as

$$\begin{aligned} R_k &= Z_{e,k} + W_{g,k} \\ &= X_{\mathrm{av},k} + \frac{1}{2}Y_k + C_{\mathrm{aco},k} + W_{g,k},\ 0 \leqslant k \leqslant N-1, \end{aligned} \tag{13}$$

where $Z_{e,k}$, $X_{\mathrm{av},k}$, $C_{\mathrm{aco},k}$ and $W_{g,k}$ are the Fourier transforms of $z_{e,n}$, $x_{\mathrm{av},n}$, $c_{\mathrm{aco},n}$ and $w_{g,n}$, respectively.

Since $\{x_{\mathrm{av},n}\}$ have the symmetry property, we have

$$\begin{aligned} X_{\mathrm{av},k} &= \frac{1}{\sqrt{N}}\sum_{n=0}^{N-1} x_{\mathrm{av},n}\exp\left(-\mathrm{j}\frac{2\pi}{N}nk\right) \\ &= \frac{1}{\sqrt{N}}\sum_{n=0}^{N/2-1} x_{\mathrm{av},n}\left(\exp\left(-\mathrm{j}\frac{2\pi}{N}nk\right)\right. \\ &\quad \left.+\exp\left(-\mathrm{j}\frac{2\pi}{N}(n+\frac{N}{2})k\right)\right) \\ &= \frac{1}{\sqrt{N}}\sum_{n=0}^{N/2-1} x_{\mathrm{av},n}\exp\left(-\mathrm{j}\frac{2\pi}{N}nk\right)(1+\cos(k\pi)). \end{aligned} \tag{14}$$

When k is odd, we have $X_{\mathrm{av},k} = 0$, which means that $X_{\mathrm{av},k}$ comprises the even subcarriers only and the transmission of ACO-OFDM symbols are not affected by the AV-DCO-OFDM parts. Note that $C_{\mathrm{aco},k}$ also comprises only the even subcarriers[8,11]. After N-point FFT and equalization, we could estimate the ACO-OFDM symbols on the odd subcarriers using ML (Maximum-Likelihood) detection, given by

$$\begin{aligned} \widehat{Y}_k &= \arg\max_{Y\in\Omega_Y} P_Y\{\widehat{R}_k|\Omega_Y\} \\ &= \arg\min_{Y\in\Omega_Y} \left\|Y - 2\widehat{R}_k\right\|_F^2,\ k = 1,3,\cdots,N/2-1, \end{aligned} \tag{15}$$

where Ω_Y denotes the constellation set of Y_k, $\widehat{R}_k$ denotes the estimation of R_k, and $\|\cdot\|_F$ denotes the Frobenius norm. The multiplication by 2 is to compensate the clipping loss according to Eq. (13).

The ACO-OFDM time-domain signal estimations $\{\widehat{y}_{\mathrm{aco},n}\}$ are then reconstructed and removed from the received signals, leading to the estimations of $\{\widehat{x}_{\mathrm{av},n}\}$. Since $\{\widehat{x}_{\mathrm{av},n}\}$ are disturbed by the ACO-OFDM estimation error and a part of the AWGN,

some parts of $\{\widehat{x}_{\mathrm{av},n}\}$ could be negative, and $\{\widehat{x}^c_{\mathrm{av},n}\}$ could be obtained by clipping the negative parts of $\{\widehat{x}_{\mathrm{av},n}\}$.

After that, we could obtain the signs of $\{x_{d,n}\}$ by using the ISEA algorithm developed in Ref. [12]. More specifically, in the ith iteration, we have

$$\widehat{x}^{c,i}_{d,n} = s^i_n \widehat{x}^c_{\mathrm{av},n}, \quad n = 1, 2, \cdots, N-1, \tag{16}$$

where s^i_n is the sign estimation of $x_{d,n}$, which is initialized to 1 before iteration for the sake of convergence, i.e., $s^0_n = 1$.

Then $\{\widehat{x}^{c,i}_{d,n}\}$ are transformed by the N-point FFT leading to $\{\widehat{\widehat{X}}^i_k\}$. The $\{\widehat{X}^i_k\}$ could be estimated by using the ML detection, which are given by

$$\begin{aligned}\widehat{X}^i_k &= \arg\max_{X\in\Omega_X} P_X\{\widehat{\widehat{X}}^i_k|\Omega_X\} \\ &= \arg\min_{X\in\Omega_X} \|X - \widehat{\widehat{X}}^i_k\|^2_F, \ k = 2, 4, \cdots, N/2-2,\end{aligned} \tag{17}$$

where Ω_X is the constellation set of X_k.

Using $\{\widehat{X}^i_k\}$, we could reconstruct the local estimations $\{\widehat{x}^i_{d,n}\}$, and update the sign estimations by

$$s^{i+1}_n = \mathrm{sign}\{\widehat{x}^i_{d,n}\} = \begin{cases} -1, & \widehat{x}^i_{d,n} < 0, \\ 1, & \widehat{x}^i_{d,n} \geqslant 0. \end{cases} \tag{18}$$

The receiver will go to the $(i+1)$th iteration until $s^i_n = s^{i-1}_n$ $(i > 0,\ n = 1, 2, \cdots, N-1)$ or i strikes the preset maximum iteration number I_M.

3 Signal analysis

3.1 PDF of the time-domain signals

The EADO-OFDM signals can be studied comprehensively using their PDF, which is investigated in this subsection. According to the central limit theorem, the bipolar time-domain signals x_n and y_n follow a Gaussian distribution with zero mean, especially for large subcarrier numbers when $N \geqslant 128$[9,13]. We assume that $x_{\mathrm{av}}(t)$ denotes the output continuous-time analog signal of D/A for the input $x_{\mathrm{av},n}$. After absolute value operation, the PDF of the AV-DCO-OFDM time-domain signals $x_{\mathrm{av}}(t)$ could easily be derived as

$$\begin{aligned}f_{x_{\mathrm{av}}(t)}(s) = &\frac{1}{\sqrt{2\pi}\sigma_D}\exp\left(\frac{-(s-B_{\mathrm{DC}})^2}{2\sigma_D^2}\right)u(s) \\ &+ \frac{1}{\sqrt{2\pi}\sigma_D}\exp\left(\frac{-(s+B_{\mathrm{DC}})^2}{2\sigma_D^2}\right)u(s),\end{aligned} \tag{19}$$

where σ_D is the standard deviation of the signals x_n. $u(s)$ is a unit step function and $u(0)$ is defined to be $1/2$ in this paper.

We can calculate the average optical power and electrical power of AV-DCO-OFDM as

$$P_{o,\mathrm{av}} = E\{x_{\mathrm{av}}(t)\} = \int_0^{+\infty} s f_{x_{\mathrm{avo}}(t)}(s)\mathrm{d}s = A(\mu)\sigma_D, \tag{20}$$

and

$$P_{e,\mathrm{av}} = E\{x^2_{\mathrm{av}}(t)\} = \int_0^{+\infty} s^2 f_{x_{\mathrm{av}}(t)}(s)\mathrm{d}s = B(\mu)\sigma_D^2, \tag{21}$$

where

$$\begin{aligned}A(\mu) &= \mu - 2\mu Q(\mu) + \frac{2}{\sqrt{2\pi}}\exp\left(-\frac{\mu^2}{2}\right), \\ B(\mu) &= 1 + \mu^2 + 4Q(\mu)\end{aligned}$$

and

$$Q(\xi) = \frac{1}{\sqrt{2\pi}}\int_\xi^\infty \exp\left(\frac{-x^2}{2}\right)\mathrm{d}x.$$

Besides, the PDF of $y_{\mathrm{aco},n}$ is given by[11]

$$f_{y_{\mathrm{aco}}(t)}(\nu) = \frac{1}{\sqrt{2\pi}\sigma_A}\exp\left(\frac{-\nu^2}{2\sigma_A^2}\right)u(\nu) + \frac{1}{2}\delta(\nu), \tag{22}$$

where σ_A is the standard deviation of y_n, and $\sigma_A = \sqrt{E\{y_n^2\}}$. $\delta(\nu)$ is the Dirac delta function. In addition, $y_{\mathrm{aco}}(t)$ denotes the output analog signal of D/A for the input $y_{\mathrm{aco},n}$. The average optical and electrical power of ACO-OFDM time-domain signals are given by $P_{o,\mathrm{aco}} = \sigma_A/\sqrt{2\pi}$ and $P_{e,\mathrm{aco}} = \sigma_A^2/2$, respectively[11].

Theorem 1 The PDF of the EADO-OFDM time-domain signals can be derived by using convolution, which is given by

$$\begin{aligned}&f_{z_e(t)}(z) \\ &= \frac{1}{2\sqrt{2\pi}\sigma_D}\left(\exp\left(\frac{-(z-B_{\mathrm{DC}})^2}{2\sigma_D^2}\right)\right.\end{aligned}$$

$$+\exp\left(\frac{-(z+B_{\mathrm{DC}})^2}{2\sigma_D^2}\right)\Bigg)$$
$$+\frac{1}{\sqrt{2\pi}\sigma}\exp\left(\frac{-(z-B_{\mathrm{DC}})^2}{2\sigma^2}\right)$$
$$\times\left(Q(\frac{\Phi(z)}{\sigma\sigma_A\sigma_D})-Q(\frac{\Delta(z)}{\sigma\sigma_A\sigma_D})\right)$$
$$+\frac{1}{\sqrt{2\pi}\sigma}\exp\left(\frac{-(z+B_{\mathrm{DC}})^2}{2\sigma^2}\right)$$
$$\times\left(Q(\frac{\Theta(z)}{\sigma\sigma_A\sigma_D})-Q(\frac{\Lambda(z)}{\sigma\sigma_A\sigma_D})\right),\quad z>0, \tag{23}$$

where $\Phi(z)=-z\sigma_D^2-B_{\mathrm{DC}}\sigma_A^2$, $\Delta(z)=z\sigma_A^2-B_{\mathrm{DC}}\sigma_A^2$, $\Theta(z)=-z\sigma_D^2+B_{\mathrm{DC}}\sigma_A^2$, $\Lambda(z)=z\sigma_A^2+B_{\mathrm{DC}}\sigma_A^2$, and $\sigma=\sqrt{\sigma_A^2+\sigma_V^2}$.

Proof See Appendix A.

Fig. 3 depicts the theoretical and simulated PDF results of the EADO-OFDM, where the average total optical power is set to unity and equal optical power allocation is used between ACO-OFDM and AV-DCO-OFDM. $M_1=16$, $M_2=16$, $\mu=2.3$, and N is set to 1 024. It is shown that the simulation results are in good agreement with the theoretical analysis.

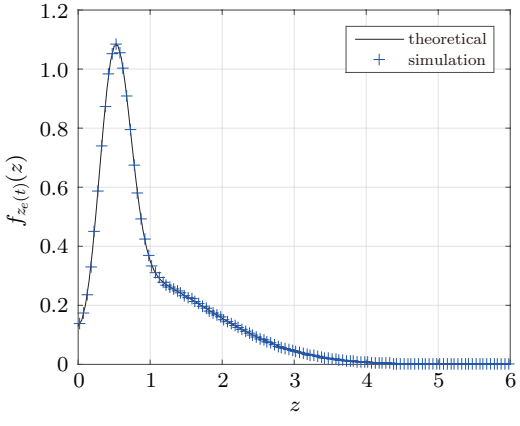

Figure 3 Theoretical and simulated PDFs of the EADO-OFDM

Theorem 2 The average optical and electrical powers of the EADO-OFDM time-domain signals are respectively given by

$$P_{o,\mathrm{eado}}=A(\mu)\sigma_D+\frac{\sigma_A}{\sqrt{2\pi}}, \tag{24}$$

and

$$P_{e,\mathrm{eado}}=\sigma_D^2B(\mu)+\frac{\sigma_A^2}{2}+\frac{2A(\mu)\sigma_A\sigma_D}{\sqrt{2\pi}}. \tag{25}$$

Proof See Appendix B.

3.2 Electrical SNR

At the receiver side, the signals after the N-point FFT could be obtained according to Eqs. (4), (9), (12), and (13) as

$$R_k=X_k+B_{DC,k}+W_{a,k}+\frac{1}{2}Y_k+C_{\mathrm{aco},k}+W_{g,k}, \tag{26}$$

where $B_{DC,k}$ and $W_{a,k}$ are the DFTs (Discrete Fourier Transforms) of B_{DC} and $w_{a,n}$, respectively. It can be confirmed that $B_{DC,k}$ comprises only the 0th subcarrier and $W_{a,k}$ comprises only the even subcarriers.

$W_{g,k}^{\mathrm{odd}}$ and $W_{g,k}^{\mathrm{even}}$ stand for the values of $W_{g,k}$ on the odd and even subcarriers, respectively. Due to the AWGN property, $W_{g,k}^{\mathrm{odd}}$ and $W_{g,k}^{\mathrm{even}}$ have the same average electrical power per symbol as $W_{g,k}$, i.e.

$$E\left\{|W_{g,k}^{\mathrm{odd}}|^2\right\}=E\left\{|W_{g,k}^{\mathrm{even}}|^2\right\}=E\left\{|W_{g,k}|^2\right\}=\sigma_g^2. \tag{27}$$

Besides, following the Parseval theorem, we have

$$\frac{1}{N}\sum_{n=0}^{N-1}|y_n|^2=\frac{1}{2}\left(\frac{1}{N/2}\sum_{m=0}^{N/2-1}|Y_{2m+1}|^2\right). \tag{28}$$

As we know, $\frac{1}{N}\sum_{n=0}^{N-1}|y_n|^2$ and $\frac{1}{N/2}\sum_{m=0}^{N/2-1}|Y_{2m+1}|^2$ are the unbiased estimators for $E\{|y_n|^2\}$ and $E\{|Y_k|^2\}$, which are the average electrical energy per symbol in the time-domain and frequency-domain for ACO-OFDM, respectively. Thus, we have

$$E\left\{|y_n|^2\right\}=\frac{1}{2}E\left\{|Y_k|^2\right\}. \tag{29}$$

Therefore, in EADO-OFDM, the electrical SNR for ACO-OFDM signals can be derived as

$$\Gamma_{\mathrm{aco}}=\frac{E\{|\frac{1}{2}Y_k|^2\}}{E\{|W_{g,k}^{\mathrm{odd}}|^2\}}=\frac{\frac{1}{2}E\{|y_n|^2\}}{E\{|W_{g,k}^{\mathrm{odd}}|^2\}}$$
$$=\frac{1}{2}\frac{\sigma_A^2}{\sigma_g^2}. \tag{30}$$

Similarly, we can derive $E\left\{|x_n|^2\right\}=\frac{1}{2}E\left\{|X_k|^2\right\}$ for AV-DCO-OFDM. As described in section 2.2,

before demodulating the AV-DCO-OFDM symbols, ACO-OFDM time-domain signal estimations of $\{\widehat{y}_{\text{aco},n}\}$ are reconstructed and removed from the received signals, and the ISEA algorithm is utilized to obtain the signal signs. Thus, the estimation errors of Y_k and the signs s_n^i could degrade the performance of AV-DCO-OFDM. Therefore, the effective SNR for AV-DCO-OFDM signals in EADO-OFDM is given by

$$\Gamma_{av} = \frac{E\left\{|X_k|^2\right\}}{E\left\{|W_{g,k}^{\text{even}}|^2\right\} + \varepsilon_e} = \frac{2\sigma_D^2}{\sigma_g^2 + \varepsilon_e}, \tag{31}$$

where ε_e denotes the equivalent degradation caused by the estimation errors of Y_k and the signal signs s_n^i. Note that when SNR is high, Y_k and s_n^i can be demodulated successfully, causing no degradation to the AV-DCO-OFDM signals, i.e., $\varepsilon_e \to 0$. Thus when SNR is high, we have

$$\Gamma_{av} \approx \frac{2\sigma_D^2}{\sigma_g^2}. \tag{32}$$

3.3 Optical power allocation

The optical power allocation between ACO-OFDM and AV-DCO-OFDM, for improving the overall performance of the EADO-OFDM, is discussed in this subsection. We assume that the average total optical power of EADO-OFDM is set to unity, and that the average optical power allocated to ACO-OFDM and AV-DCO-OFDM are α and $1-\alpha$, respectively.

Substituting $P_{o,\text{aco}} = \alpha = \sigma_A/\sqrt{2\pi}$ in Eq. (30) leads to

$$\Gamma_{\text{aco}} = \frac{\pi\alpha^2}{\sigma_g^2}. \tag{33}$$

Besides, when the SNR is high, we substitute $P_{o,\text{av}} = 1-\alpha = A(\mu)\sigma_D$ in Eq. (32), which results in

$$\Gamma_{av} = \frac{2(1-\alpha)^2}{A^2(\mu)\sigma_g^2}. \tag{34}$$

When QAM with gray labeling is used, the BER performance of ACO-OFDM and AV-DCO-OFDM in ADO-OFDM can be formulated as[14,15]

$$P_{b,\text{aco}} \approx \frac{4(\sqrt{M_1}-1)}{\sqrt{M_1}\text{lb}M_1} Q\left(\sqrt{\frac{3}{M_1-1}\Gamma_{\text{aco}}}\right) \tag{35}$$

and

$$P_{b,\text{av}} \approx \frac{4(\sqrt{M_2}-1)}{\sqrt{M_2}\text{lb}M_2} Q\left(\sqrt{\frac{3}{M_2-1}\Gamma_{av}}\right). \tag{36}$$

For high SNR and a large subcarrier number N, the overall BER performance of EADO-OFDM could be derived as[15]

$$\begin{aligned} & P_{b,\text{e-ado}} \\ \approx & \frac{4(\sqrt{M_1}-1)}{\sqrt{M_1}\text{lb}(M_1M_2)} Q\left(\alpha\sqrt{\frac{3\pi}{(M_1-1)\sigma_g^2}}\right) \\ & + \frac{4(\sqrt{M_2}-1)}{\sqrt{M_2}\text{lb}(M_1M_2)} Q\left(\frac{1-\alpha}{A(\mu)}\sqrt{\frac{6}{(M_2-1)\sigma_g^2}}\right). \end{aligned} \tag{37}$$

$P_{b,\text{e-ado}}$ is a convex function of α $(0<\alpha<1)$ for high SNR[15]. Thus, we can calculate the minimum value of $P_{b,\text{e-ado}}$ by setting its derivative function to zero,

$$P'_{b,\text{e-ado}}(\alpha) = 0. \tag{38}$$

Following (33) in Ref. [15], we can obtain an approximation of the solution to Eq. (38) for high SNR, which is given by

$$\begin{aligned} & \alpha_0^A \\ = & \frac{1}{1+A(\mu)\sqrt{\frac{\pi}{2}\frac{M_2-1}{M_1-1}}} \\ = & \frac{1}{1+\left(\mu-2Q(\mu)+\frac{2}{\sqrt{2\pi}}\exp\left(-\frac{\mu^2}{2}\right)\right)\sqrt{\frac{\pi}{2}\frac{M_2-1}{M_1-1}}}. \end{aligned} \tag{39}$$

3.4 Computational complexity analysis

At the transmitter, two N-point IFFT blocks should be used for EADO-OFDM, hence the computational complexity can be written as $2\mathcal{O}(N\text{lb}N)$[16]. The power-efficient DCO-OFDM in Ref. [12] and conventional ADO-OFDM require one and two N-point IFFT blocks, respectively, thus their computational complexity can be respectively written as $\mathcal{O}(N\text{lb}N)$ and $2\mathcal{O}(N\text{lb}N)$. At the receiver, we assume that the factual maximum iteration number is I_F, which is less than or equal to the preset maximum iteration number, i.e., $I_F \leqslant I_M$. According to Fig. 2,

one IFFT block is utilized to estimate the ACO-OFDM symbols and another one is required to reconstruct the ACO-OFDM time-domain signals, in which its computational complexity can be estimated as $2\mathcal{O}(N\text{lb}N)$. Besides, two IFFT blocks are used in each iteration of the ISEA algorithm; therefore, its computational complexity can be written as $2I_F\mathcal{O}(N\text{lb}N)$. Consequently, the overall computational complexity of the EADO-OFDM receiver can be estimated as $2(I_F+1)\mathcal{O}(N\text{lb}N)$. Similarly, for the power-efficient DCO-OFDM, the computational complexity can be estimated as $2I_F\mathcal{O}(N\text{lb}N)$. In addition, the computational complexity can be written as $3\mathcal{O}(N\text{lb}N)$ for the conventional ADO-OFDM[15].

4 Numerical results

In this section, the BER performance of EADO-OFDM is analyzed, and compared to the power-efficient DCO-OFDM in Ref. [12] and the ADO-OFDM in Ref. [11], in terms of the overall electrical SNR. The average total optical power is set to unity. For the sake of simplicity, a flat channel with AWGN and ideal time synchronization are assumed at the receiver. In addition, the FFT/IFFT size N is set to 1 024.

The theoretical and simulative BER performances of the EADO-OFDM are shown in Fig. 4, where $M_1 = M_2 = 16$, $\mu = 2.3$, and $I_M = 16$ with $\alpha_0^A = 0.26$ according to Eq. (39) or $\alpha = 0.50$ are employed. Firstly, it can be seen that the symbols modulated by EADO-OFDM could be detected successfully by the receiver. The theoretical results obtained using Eqs. (35), (36), and (37) are in good agreement with results of the simulations, especially for high SNR, which validates the discussions in sections 3.2 and 3.4. When the SNR is small, estimation errors would occur during the demodulation of ACO-OFDM symbols of Y_k and AV-DCO-OFDM signal signs of s_n^i, which cause degradation in AV-DCO-OFDM performance. Therefore, ε_e in Eq. (31) is not negligible. Besides, EADO-OFDM with $\alpha_0^A = 0.26$ according to Eq. (39) achieves 4.2 dB overall performance gain than that with $\alpha = 0.50$ at a BER of 10^{-5}. In addition, ACO-OFDM and AV-DCO-OFDM in EADO-OFDM with α_0^A have similar BER performance in the high SNR regime, which is desirable for practical optical wireless communication systems.

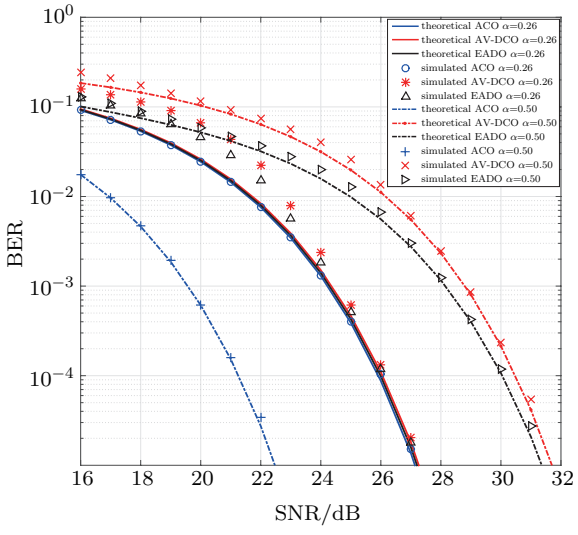

Figure 4 BER performance of the EADO-OFDM (lines show theoretical error bounds and makers simulation results)

Fig. 5 depicts the overall BER performance versus different optical power allocation factors. In case 1, 16-QAM for AV-DCO-OFDM is employed on the even subcarriers and 16-QAM for ACO-OFDM is employed on the odd subcarriers, with $\mu = 2.3$ and $I_M = 16$. In addition, the overall electrical SNR is preset to 27 dB to ensure a good performance. It can be observed that the overall BER performance of the

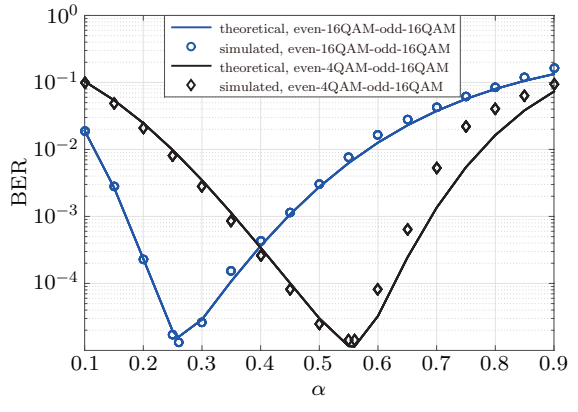

Figure 5 Overall BER performance versus different optical power allocation factors

EADO-OFDM becomes increasingly better when α increases from 0.1 to $\alpha_0^A = 0.26$, and worsens when α increases from α_0^A to 0.9. Hence, the EADO-OFDM achieves its best overall BER performance with the optical power allocation factor $\alpha_0^A = 0.26$. Similarly, in case 2 where 4-QAM for AV-DCO-OFDM and 16-QAM for ACO-OFDM are employed with $\mu = 1.3$, $I_M = 16$, and SNR = 22 dB, EADO-OFDM performs best when $\alpha_0^A = 0.56$.

In Fig. 6, the overall BER performances of the EADO-OFDM, the conventional ADO-OFDM, and the power-efficient DCO-OFDM for a spectral efficiency of $R = 3$ bit/s·Hz^{-1} are compared. For EADO-OFDM, 16-QAM is utilized for ACO-OFDM and 4-QAM is utilized for AV-DCO-OFDM, with $\mu = 1.3$ and $I_M = 16$. The optical power allocation factor $\alpha = 0.56$ is calculated according to Eq. (39). For the conventional ADO-OFDM, the same constellations are utilized with $\mu = 1.5$ to ensure good performance. In addition, the optical power allocation factor is given by $\alpha = 0.53$ according to (33) in Ref. [15]. For the power-efficient DCO-OFDM proposed in Ref. [12], 8-QAM is used with a DC bias of $\mu = 2.0$ to ensure good performance. From Fig. 6, it is evident that EADO-OFDM shows the best performance, and achieves respectively 1.8 dB and 2.0 dB performance gains compared to the conventional ADO-OFDM and the power-efficient DCO-OFDM at a BER of 10^{-5}. Specifically, when the SNR is small, EADO-OFDM performs a little worse than ADO-OFDM, because if the signal signs are demodulated incorrectly, its clipping distortion will be almost two times as that of the DCO-OFDM in the conventional ADO-OFDM according to Eq. (5). However, when the SNR is high, the signal signs could be demodulated successfully without any clipping distortion in EADO-OFDM, which makes EADO-OFDM perform better than the conventional ADO-OFDM. In addition, the constellation size combinations are more flexible and an appropriate combination can be chosen to achieve the same spectral efficiency, and the DC bias required is smaller compared to the power-efficient DCO-OFDM, which makes EADO-OFDM perform better.

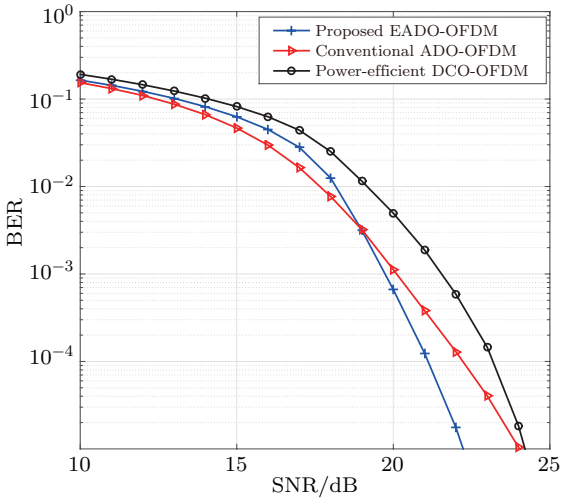

Figure 6 Overall BER performance comparison among EADO-OFDM, conventional ADO-OFDM, and power-efficient DCO-OFDM with the same spectral efficiency

5 Conclusions

In this paper, EADO-OFDM was proposed for IM/DD optical systems, in which the AV-DCO-OFDM symbols on the even subcarriers and ACO-OFDM symbols on the odd subcarriers are combined and transmitted simultaneously. Besides, we discussed the electrical SNR, optical power allocation, and computational complexity. The simulations validated the theoretical analysis and confirmed that the EADO-OFDM is an attractive solution due to its advantages. Firstly, EADO-OFDM is more energy efficient compared to the power-efficient DCO-OFDM, since the DC bias required is smaller when appropriate constellation size combinations are chosen. In addition, EADO-OFDM performs better than the conventional ADO-OFDM, because the absolute value operation causes no clipping distortion.

Appendix

A) Proof of Theorem 1

The PDF of the EADO-OFDM time-domain signals can be derived by using convolution, which is given by

$$f_{z_e(t)}(z) = \int_{-\infty}^{+\infty} f_{x_{\mathrm{aco}}(t)}(z-\lambda) f_{y_{\mathrm{av}}(t)}(\lambda) \mathrm{d}\lambda$$

$$
\begin{aligned}
&= \int_0^z \left\{ \frac{1}{\sqrt{2\pi}\sigma_A} \exp\left(\frac{-(z-\lambda)^2}{2\sigma_A^2}\right) + \frac{1}{2}\delta(z-\lambda) \right\} \\
&\quad \frac{1}{\sqrt{2\pi}\sigma_D} \left\{ \exp\left(\frac{-(\lambda - B_{\mathrm{DC}})^2}{2\sigma_D^2}\right) \right. \\
&\quad \left. + \exp\left(\frac{-(\lambda + B_{\mathrm{DC}})^2}{2\sigma_D^2}\right) \right\} \mathrm{d}\lambda \\
&= \frac{1}{2\sqrt{2\pi}\sigma_D} \left(\exp\left(\frac{-(z - B_{\mathrm{DC}})^2}{2\sigma_D^2}\right) \right. \\
&\quad \left. + \exp\left(\frac{-(z + B_{\mathrm{DC}})^2}{2\sigma_D^2}\right) \right) \\
&\quad + \frac{1}{\sqrt{2\pi\sigma}} \exp\left(\frac{-(z - B_{\mathrm{DC}})^2}{2\sigma^2}\right) \\
&\quad \times \left(Q\left(\frac{\Phi(z)}{\sigma\sigma_A\sigma_D}\right) - Q\left(\frac{\Delta(z)}{\sigma\sigma_A\sigma_D}\right) \right) \\
&\quad + \frac{1}{\sqrt{2\pi\sigma}} \exp\left(\frac{-(z + B_{\mathrm{DC}})^2}{2\sigma^2}\right) \\
&\quad \times \left(Q\left(\frac{\Theta(z)}{\sigma\sigma_A\sigma_D}\right) - Q\left(\frac{\Lambda(z)}{\sigma\sigma_A\sigma_D}\right) \right), \quad z > 0, \quad (40)
\end{aligned}
$$

where we define

$$
\begin{aligned}
\Phi(z) &= -z\sigma_D^2 - B_{\mathrm{DC}}\sigma_A^2, \\
\Delta(z) &= z\sigma_A^2 - B_{\mathrm{DC}}\sigma_A^2, \\
\Theta(z) &= -z\sigma_D^2 + B_{\mathrm{DC}}\sigma_A^2, \\
\Lambda(z) &= z\sigma_A^2 + B_{\mathrm{DC}}\sigma_A^2, \\
\sigma &= \sqrt{\sigma_A^2 + \sigma_V^2}.
\end{aligned}
$$

B) Proof of Theorem 2

The average optical power of the EADO-OFDM signals is given by

$$
\begin{aligned}
P_{o,\mathrm{eado}} &= E\{z_e(t)\} \\
&= E\{x_{\mathrm{avo}}(t) + y_{\mathrm{aco}}(t)\} \\
&= A(\mu)\sigma_D + \frac{\sigma_A}{\sqrt{2\pi}}. \qquad (41)
\end{aligned}
$$

Since $x_{\mathrm{avo}}(t)$ and $y_{\mathrm{aco}}(t)$ are statistically independent, the average electrical power of the EADO-OFDM signals can be derived by

$$
\begin{aligned}
P_{e,\mathrm{eado}} &= E\{z_e^2(t)\} = E\{(x_{\mathrm{avo}}(t) + y_{\mathrm{aco}}(t))^2\} \\
&= E\{x_{\mathrm{avo}}^2(t)\} + E\{y_{\mathrm{aco}}^2(t)\} \\
&\quad + 2E\{x_{\mathrm{avo}}(t)y_{\mathrm{aco}}(t)\} \\
&= \sigma_D^2 B(\mu) + \frac{\sigma_A^2}{2} + \frac{2A(\mu)\sigma_A\sigma_D}{\sqrt{2\pi}}. \qquad (42)
\end{aligned}
$$

References

[1] P. H. Pathak, X. T. Feng, P. F. Hu, et al. Visible light communication, networking, and sensing: a survey, potential and challenges [J]. IEEE communications surveys & tutorials, 2015, 17(4): 2047-2077.

[2] C. Gong, S. B. Li, Q. Gao, et al. Power and rate optimization for visible light communication system with lighting constraints [J]. IEEE transactions on signal processing, 2015, 63(16): 4245-4256.

[3] J. Zhou, Y. Yan, Z. Cai, et al. A cost-effective and efficient scheme for optical OFDM in short-range IM/DD systems [J]. IEEE photonics technology letters, 2014, 26(13): 1372-1374.

[4] G. Pedersen. Amplitude modulated RF fields stemming from a GSM/DCS-1800 phone [J]. Wireless networks, 1997, 3(6): 489-498.

[5] A. Chubukjian, J. Benger, R. Otnes, et al. Potential effects of broadband wireline telecommunications on the HF spectrum [J]. IEEE communications magazine, 2008, 46(11): 49-54.

[6] J. Zhou, Y. J. Qiao, T. T. Zhang, et al. FOFDM based on discrete cosine transform for intensity-modulated and direct-detected systems [J]. Journal of lightwave technology, 2016, 34(16): 3717-3725.

[7] R. Zhang, L. Hanzo. Multi-layer modulation for intensity-modulated direct-detection optical OFDM [J]. Journal of optical communications and networking, 2013, 5(12): 1402-1412.

[8] J. Armstrong, A. J. Lowery. Power efficient optical OFDM [J]. Electronics letters, 2006, 42(6): 370-372.

[9] J. Armstrong. OFDM for optical communications [J]. Journal of lightwave technology, 2009, 27(3): 189-204.

[10] S. D. Dissanayake, K. Panta, J. Armstrong. A novel technique to simultaneously transmit ACO-OFDM and DCO-OFDM in IM/DD systems [C]//IEEE Global Communications Conference, 2011: 782-786.

[11] S. D. Dissanayake, J. Armstrong. Comparison of ACO-OFDM, DCO-OFDM and ADO-OFDM in IM/DD systems [J]. Journal of lightwave technology, 2013, 31(7): 1063-1072.

[12] A. Weiss, A. Yeredor, M. Shtaif. Iterative symbol recovery for power-efficient DC-biased optical OFDM systems [J]. Journal of lightwave technology, 2016, 34(9): 2331-2338.

[13] J. Wang, Y. Xu, X. Ling, et al. PAPR analysis for OFDM visible light communication [J]. Optics express, 2016, 24(24): 27457-27474.

[14] J. Li, X. D. Zhang, Q. B. Gao, et al. Exact BEP analysis for coherent M-ary PAM and QAM over AWGN and Rayleigh fading channels [C]//IEEE Vehicular Technology Conference, Singapore, 2008: 390-394.

[15] R. W. Bai, R. Jiang, T. Q. Mao, et al. Iterative receiver for ADO-OFDM with near-optimal optical power allocation [J]. Optics communications, 2017, 387: 350-356.

[16] A. V. Oppenheim, R. W. Schafer, J. R. Buck. Discrete-time signal processing [M]. New Jersey: Printice Hall Inc., 1989.

About the authors

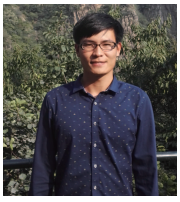

Ruowen Bai [corresponding author] received his B.E. degree from Nankai University, China, in 2015. He is currently working towards his M.E. degree at Tsinghua National Laboratory for Information Science and Technology, Department of Electronic Engineering, Tsinghua University. His research interest includes visible light communications. (Email: brw15@mails.tsinghua.edu.cn)

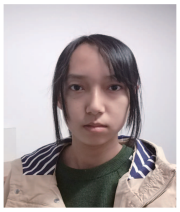

Jiaxuan Chen received her B.E. degree from Tsinghua University, Beijing, China, in 2016. She is currently working towards her Ph.D degree at Tsinghua National Laboratory for Information Science and Technology, Department of Electronic Engineering, Tsinghua University. Her research interest includes visible light communications. (Email: chenjx16@mails.tsinghua.edu.cn)

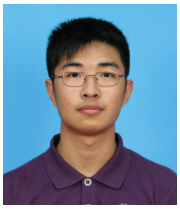

Tianqi Mao received his B.S. degree in 2015 from Tsinghua University, Beijing, China, where he is currently working towards his M.S. degree with the Department of Electronic Engineering. His current research interests include optical wireless communications and channel coding and modulation. (Email: Mtq15@mails.tsinghua.edu.cn)

Zhaocheng Wang received his B.S., M.S., and Ph.D. degrees from Tsinghua University, Beijing, China, in 1991, 1993, and 1996, respectively. From 1996 to 1997, he was a postdoctoral fellow with Nanyang Technological University, Singapore. From 1997 to 1999, he was with OKI Techno Centre (Singapore) Pte. Ltd., Singapore, where he was first a research engineer and later became a senior engineer. From 1999 to 2009, he was with Sony Deutschland GmbH, where he was first a senior engineer and later became a principal engineer. He is currently a professor of Electronic Engineering with Tsinghua University and serves as the director of Broadband Communication Key Laboratory, Tsinghua National Laboratory for Information Science and Technology (TNlist). He has authored or coauthored over 120 journal papers. He is the holder of 34 granted U.S./EU patents. He coauthored two books, one of which, Millimeter wave communication systems, was selected by IEEE Series on Digital and Mobile Communication (Wiley-IEEE Press). His research interests include wireless communications, visible light communications, millimeter wave communications, and digital broadcasting. He is a fellow of the Institution of Engineering and Technology. He served as the associate editor of IEEE transactions on wireless communications (2011-2015) and the associate editor of IEEE communications letters (2013-2016), and has also served as technical program committee co-chair of various international conferences. (Email: zcwang@tsinghua.edu.cn)